Journal of Alloys and Compounds 509 (2011) 4452–4456

Contents lists available at ScienceDirect

Journal of Alloys and Compounds

journal homepage: www.elsevier.com/locate/jallcom

$K_3BiAs_6Se_{12}$: A two-dimensional bismuth selenoarsenate containing crown-shaped anions $[As_3Se_6]^{3-}$

Yuandong Wu, Wolfgang Bensch*

Institut für Anorganische Chemie, Universität Kiel, Max-Eyth-Str. 2, D-24118 Kiel, Germany

ARTICLE INFO

Article history:
Received 28 October 2010
Received in revised form 10 January 2011
Accepted 16 January 2011
Available online 22 January 2011

Keywords:
Alkali polyselenoarsenate flux
Bismuth selenoarsenate
Crystal structure
Spectroscopic properties

ABSTRACT

Single crystals of $K_3BiAs_6Se_{12}$ were obtained from the reaction of Bi, with in situ formed fluxes of K_2Se_3, As_2Se_3, and Se at 500 °C. The compound crystallizes in the trigonal space group $P\,\overline{3}$ (No. 147) with $a = 9.7478(7)$, $c = 7.6525(6)$ Å, $V = 629.72(8)$ Å^3, $Z = 1$. The $[Bi(As_3Se_6)_2]^{3-}$ anion possesses a two-dimensional layered structure with trigonal symmetry consisting of $[BiSe_6]$ octahedra and crown-like cyclic $[As_3Se_6]^{3-}$ units formed by three corner-sharing trigonal pyramidal $[AsSe_3]^{3-}$ anions. The $[As_3Se_6]^{3-}$ fragment is located on a 3-fold axis with three As atoms and three Se atoms forming a six-membered ring in chair conformation. The Bi^{3+} ion is in an almost perfect octahedral geometry. The overall arrangement of the Bi^{3+} cations and the $[As_3Se_6]^{3-}$ anions is related to the CdI_2-type structure with the cations situated on the Cd^{2+} and the anions on the I^- sites, respectively.

The K^+ cations are located between the $[Bi(As_3Se_6)_2]^{3-}$ layers. The $K(1)^+$ cation is coordinated by 9 Se^{2-} anions from four $[As_3Se_6]^{3-}$ units, one above and three below, in an irregular geometry, whereas the $K(2)^+$ cation is surrounded by six Se^{2-} anions from four $[As_3Se_6]^{3-}$ units, two above and two below, in a perfect octahedral fashion. The title compound is characterized with UV/vis diffuse reflectance spectroscopy, IR and Raman spectra.

1. Introduction

The growing class of quaternary phases containing various group 15/16 anions is now a substantial subclass of solid state chalcogenides [1]. Among these compounds, chalcogeno-arsenates, although limited in number, show a variety of structures and different anionic $[As_xQ_y]^{n-}$ (Q = S, Se) building units. The most dominant anions are the pyramidal $[As^{III}Q_3]^{3-}$ and tetrahedral $[As^{V}Q_4]^{3-}$ anions, observed in ternary or quaternary compounds [2–24]. Other anionic variations include pyramidal $[As^{III}Q_4]^{3-}$ and $[As^{III}Q_5]^{3-}$ [25], which contain Q–Q dumbbells, and their condensed oligomeric forms such as $[As_2Q_5]^{4-}$ [12], $[As_3Q_6]^{3-}$ [12,18], and $[As_4Q_8]^{4-}$ [14] anions. The structures containing $[As^{III}Q_3]_n{}^{3-}$ ($n = 2, 3, 4$) units are expected to exhibit a unique structural chemistry due to the stereochemically active As^{III} $4s^2$ lone pair.

Until now the most successful synthetic approach for the formation of ternary or quaternary chalcogenoarsenates has been the hydro- (solvento-) thermal technique. However, little work about polychalcogenoarsenate fluxes has been reported. Recently we have reported several quaternary rare earth chalcogenoarsenates, $K_3Ln(AsS_4)_2$ (Ln = Nd, Sm Gd, Dy) [26,27], $KEuAsS_4$, and $Rb_4Nd_{0.67}(AsS_4)_2$ [27], $K_2Ln_2As_2Se_9$ (Ln = Sm, Gd) [28] prepared in polychalcogenoarsenate fluxes. In this case, one feature that seems to be evident in this type of chemistry is that the reactivity of arsenic in alkali polysulfide fluxes differs significantly from that in polyselenide fluxes. As in selenoarsenates favor predominantly the +3 state, whereas the +5 state is more stable in thioarsenates as proved by the frequent occurrence of the $[AsS_4]^{3-}$ anion. This difference is due to the different chemical reactivity of these fluxes. The considerable structural diversity in the class of chalcogenoarsenate compounds is attributed to various binding modes and reactivities of chalcogenoarsenate anions in the molten flux to coordinate lanthanoide metals [26–28]. Other reaction systems like A-M-As-Q (A = alkali metals, M = Ga, In, Bi, Q = S, Se) are also very interesting because the influence of the size of the cations and of the stereoactivity of the lone electron pairs can be studied. Three compounds $(Ph_4P)_2In(As_3S_7)$ and $(Me_4N)_2RbBi(As_3S_6)_2$ [18] and $Cs_4BiAs_3Se_7$ [29] have been reported in these chalcogenoarsenate systems, which were prepared via solvothermal reaction and contain $[InAs_3S_7]^{2-}$ and $[BiAs_3Se_7]^{4-}$ chains resp. the $[Bi(As_3S_6)_2]^{3-}$ layer anion. Here, we report the result of the polyselenoarsenate flux synthesis within the K–Bi–As–Se system and present the structure and selected properties of the new bismuth selenoarsenate $K_3BiAs_6Se_{12}$. The compound contains infinite layer anions $[Bi(As_3Se_6)_2]^{3-}$ and adopts the space group $P\,\overline{3}$ that arises from the alignment of the $[As_3Se_6]^{3-}$ ring anions.

---

* Corresponding author. Tel.: +49 431 880 2091; fax: +49 431 880 1520.
E-mail address: wbensch@ac.uni-kiel.de (W. Bensch).

0925-8388/$ – see front matter © 2011 Elsevier B.V. All rights reserved.
doi:10.1016/j.jallcom.2011.01.108

2. Experimental

2.1. Reagents

The reagents employed in this work were used as obtained: K metal, 99.95%, ABCR; Bi powder, -100 mesh, 99.99%, Chempur; Se powder, -200 mesh, 99.5%, Retorte; As_2Se_3, 99.999%, ABCR; *N,N*-dimethylformamide (DMF), industrial reagent grade, BASF; diethylether, analytical reagent grade, anhydrous, 99.8%, Fluka. The K_2Se_3 starting material was prepared by reacting stoichiometric amounts of the elements in liquid ammonia in an argon atmosphere.

2.2. Synthesis

$K_3BiAs_6Se_{12}$ was prepared by reacting a mixture of K_2Se_3, Bi, As_2Se_3, and additional Se powder in a 1:1:1.5:2 molar ratio. The mixture was thoroughly mixed in a N_2-filled glove box and loaded into a glass ampoule. After evacuation to $\sim 10^{-3}$ mbar the ampoule was flame sealed and placed in a computer-controlled furnace. The mixture was heated to 540 °C at a rate of 0.5 °C/min, kept at this temperature for 5 days before the sample was cooled down to 100 °C at a rate of 3 °C/h, then the furnace was switched off to cool to room temperature. The product was washed with dry *N,N*-dimethylformamide and diethylether yielding black platelets (yield about 40% based on Bi). The single crystals are stable in DMF, pure ethanol, dry air for up to two months. EDX analyses performed on freshly cleaved faces of several crystals indicated the presence of all four elements (K, Bi, As, Se) and for all crystals the average composition is $K_{2.6}BiAs_{6.0}Se_{12.5}$. The synthesis of pure $K_3BiAs_6Se_{12}$ was unsuccessful until now. Attempts to replace potassium with rubidium or cesium resulted in mixtures of binary and ternary compounds, namely Bi_2Se_3, ABi_4Se_7 (A = Rb, Cs) [30].

2.3. Crystal structure determination

A black plate-shaped crystal with dimensions of 0.14 × 0.10 × 0.06 mm^3 was manually selected and then mounted on the top of a glass fiber. Single crystal X-ray diffraction data were collected with graphite-monochromstized Mo $K\alpha$ radiation (λ = 0.71073 Å) at 293 K on a STOE Imaging Plate Diffraction System (IPDS-1). The raw intensities were treated in the usual way applying Lorentz, polarization, and numerical absorption corrections.

The lattice parameters pointed toward the hexagonal or trigonal crystal system and the space group $P\,\overline{3}$ was selected. The structure model was obtained by direct methods and was refined by full-matrix least-squares refinement based on F^2 using the SHELXTL package [31]. The positions were standardized with the STRUCTURE TIDY program within the PLATON package [32]. The final refinement converged with a residual factor of wR_2 = 0.095(all data). Technical details of the data acquisition as well as some refinement results are summarized in Table 1. Atomic coordinates and equivalent isotropic displacement parameters are given in Table 2. Selected bond lengths and angles are listed in Table 3.

Further details of the crystal structure investigation can be ordered referring to the depository No CSD-422567, the authors and the citation of this paper at the Fachinformationszentrum Karlsruhe, Gesellschaft für wissenschaftlich- technische Information mbH. D-76344 Eggenstein-Leopoldshafen (Germany). E-mail: crysdata@fiz-karlsruhe.de

2.4. Physical measurements

2.4.1. Infrared spectroscopy

Infrared spectrum in the MIR region (4000–400 cm^{-1}, 2 cm^{-1} resolution) was recorded on a Genesis FT-spectrometer (ATI Mattson). The sample was ground with dry KBr into fine powder and pressed into transparent pellet. Infrared spectrum in the far-IR region (550–80 cm^{-1}) was collected on an ISF-66 device (Bruker) with the sample pressed in a polyethylene pellet.

2.4.2. Raman spectroscopy

The Raman spectrum was recorded on an ISF-66 spectrometer (Bruker) equipped with an additional FRA 106 Raman module. A Nd/YAG laser was used as source (λ = 1064 nm). The sample was ground and prepared on an Al sample holder. The measuring range was −1000 to 3500 cm^{-1} (resolution: 2 cm^{-1}).

2.4.3. Solid-state ultraviolet (UV)–visible(vis)-near-IR spectroscopy

Optical diffuse reflectance measurement was performed at room temperature using a UV–vis-NIR two-channel spectrometer Cary 5 from Varian Techtron Pty., Darmstadt. The spectrometer is equipped with an Ulbricht sphere (Diffuse reflectance accessory; Varian Techtron Pty.). The inner wall of the Ulbricht sphere (diameter 110 mm) is covered with a PTFE layer of 4 mm thickness. A PbS detector (NIR) and a photomultiplier (UV/Vis) are attached to the Ulbricht sphere. The sample was ground with $BaSO_4$ (as standard for 100% reflectance) and prepared as a flat specimen. The resolution was 1 nm for the UV/Vis range and 2 nm for the near-IR range. The measuring range was 250–2000 nm. Absorption (α/S) data were calculated from the reflectance spectra using the Kubelka–Munk function [33]: $\alpha/S = (1-R)^2/2R$, where R is the reflectance at a given wave-number, α is the absorption coefficient, and S is the scattering coefficient. The band gap was determined as the intersection point between the energy axis at the absorption offset and the line extrapolated from the linear part of the absorption edge in a $(\alpha/S)^2$ vs. E (eV) plot.

Table 1
Technical details of data acquisition and some refinement results for $K_3BiAs_6Se_{12}$.

Empirical formula	$K_3BiAs_6Se_{12}$
Formula weight (g/mol)	1723.32
Temperature (K)	293
Wavelength (Å)	0.71073
Crystal system	Trigonal
Space group	$P\,\overline{3}$ (no. 147)
a/Å	9.7478(7)
c/Å	7.6525(6)
V/Å^3	629.72(8)
Z	1
Calc. density (g cm^{-3})	4.544
Crystal color	Black
μ/mm^{-1}	32.648
F(0 0 0)	746
Crystal size (mm^3)	0.14 × 0.10 × 0.06
2θ range	$5^\circ \leq 2\theta \leq 56^\circ$
Index range	$-11 \leq h \leq 12$ $-12 \leq k \leq 12$ $-10 \leq l \leq 10$
Reflections collected	5298
Independent reflections	1016
R_{int}	0.0946
Completeness to θ = 27.91°	99.7%
Refinement method	Full-matrix least square on F^2
Min./max. transm.	0.0152/0.0694
Refl. with $F_o > 4\sigma(F_o)$	943
Number of parameters	36
Goodness-of-fit on F^2	1.117
Final R for $F_o > 4\sigma(F_o)$[a,b]	$R_1 = 0.0361$, $wR_2 = 0.0930$
R indices for all reflections[a,b]	$R_1 = 0.0393$, $wR_2 = 0.0950$
$\Delta\rho$ [e Å^{-3}]	2.758/−2.419

[a] $R_1 = \Sigma||F_o|-|F_c||/\Sigma|F_o|$

[b] $wR_2 = [\Sigma w((F_o{}^2 - F_c{}^2)^2/\Sigma w(F_o{}^2)^2]^{1/2}$, $w = 1/\Sigma(F_o{}^2) + (aP)2 + bP]$, where $P = (\max(F_o{}^2, 0) + 2F_c{}^2)/3$

Table 2
Atomic coordinates and equivalent isotropic displacement parameters U_{eq} (Å^2 × 10^3) for $K_3BiAs_6Se_{12.}$ Estimated standards deviations are given in parentheses. The U_{eq} is defined as one third of the trace of the orthogonalized U_{ij} tensor.

	x	y	z	U_{eq}
Bi	0	0	$^1/_2$	14(1)
Se(1)	0.5329(1)	0.9052(1)	0.1969(1)	21(1)
Se(2)	0.2739(1)	0.0605(1)	0.2791(1)	21(1)
As	0.2978(1)	0.8436(1)	0.3691(1)	18(1)
K(1)	$^1/_3$	$^2/_3$	0.8278(5)	36(1)
K(2)	0	0	0	45(1)

Table 3
Selected bond distances (Å) and angels (°) for $K_3BiAs_6Se_{12.}$ Estimated standard deviations are given in parentheses.

Bi–Se(2)	2.9599(7) × 4	Bi–Se(2)	2.9600(7) × 2
Se(1)–As	2.4317(10)	Se(1)–As	2.4437(10)
Se(2)–As	2.3436(9)	K(1)–Se(2)	3.4953(12) × 2
K(1)–Se(2)	3.4954(12)	K(1)–Se(1)	3.556(3) × 2
K(1)–Se(1)	3.7033(8)	K(1)–Se(1)	3.7034(8) × 2
K(2)–Se(2)	3.2348(8) × 6		
Se(2)–Bi–Se(2)	90.61(2) × 6		
Se(2)–Bi–Se(2)	89.39(2) × 6		
Se(2)–Bi–Se(2)	180.0 × 6		
Se(2)–As–Se(1)	102.48(4)		
Se(2)–As–Se(1)	97.12(3)		
Se(1)–As–Se(1)	100.25(4)		
As–Se(1)–As	86.06(4)		
As–Se(2)–Bi	98.01(3)		

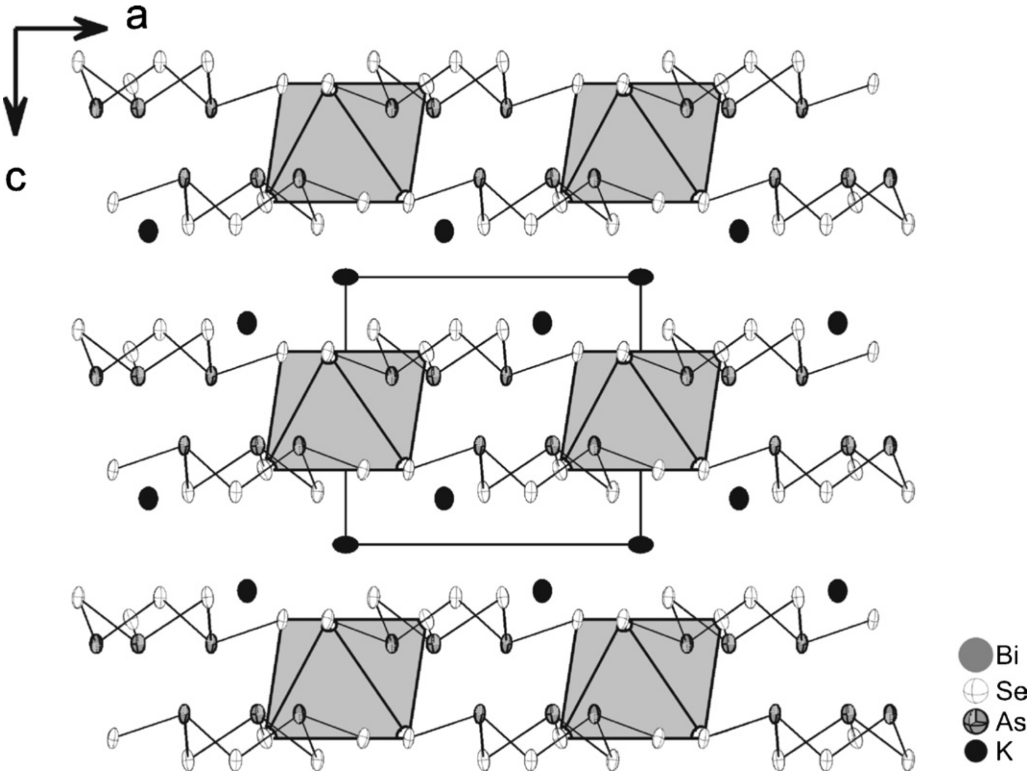

Fig. 1. Crystal structure of $K_3BiAs_6Se_{12}$ viewed along [0 1 0]. The $[BiSe_6]$ octahedra are displayed as polyhedra for clarity. The displacement ellipsoids are drawn at the 50% probability level.

3. Results and discussion

3.1. Crystal structure

The new quaternary bismuth selenoarsenate $K_3BiAs_6Se_{12}$ crystallizes in the trigonal space group $P\overline{3}$ with one crystallographically independent Bi, one As, two unique K and Se atoms. The crystal structure is composed of $^{2}{}_{\infty}[BiAs_6Se_{12}]^{3-}$ anionic layers which are well separated by the K^+ cations (Fig. 1).

The layer $^{2}{}_{\infty}[BiAs_6Se_{12}]^{3-}$ is built up of Bi^{3+} cations and $[As_3Se_6]^{3-}$ units. (Fig. 2). The $[As_3Se_6]^{3-}$ anion consists of a six-membered As_3Se_3 ring in chair conformation, with alternating As

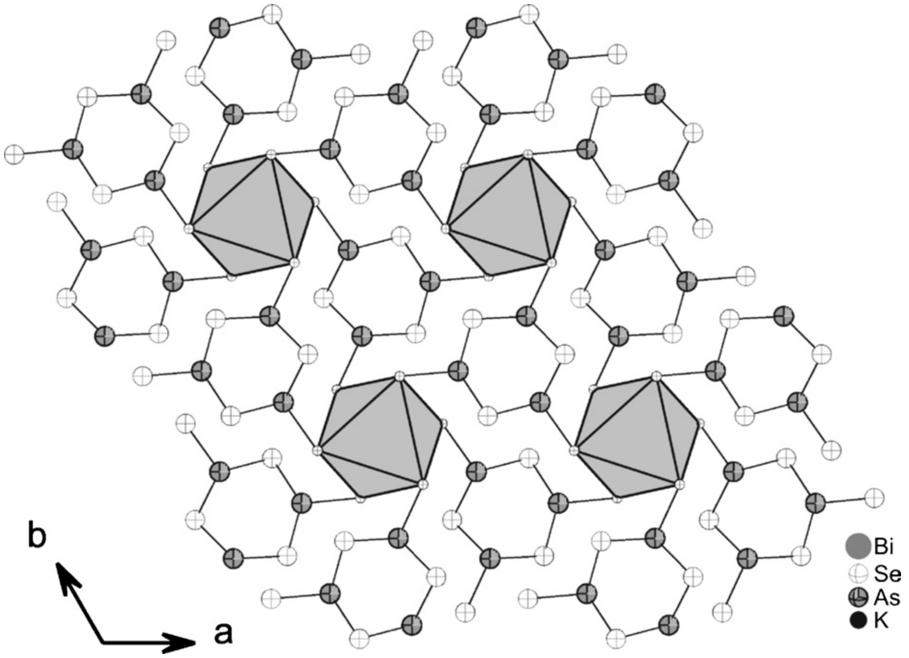

Fig. 2. View of one $^{2}{}_{\infty}[Bi(As_3Se_6)_2]^{3-}$ layer down the [0 0 1] direction.

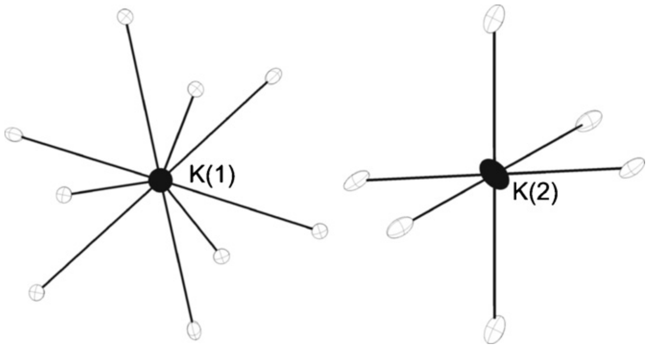

Fig. 3. Coordination of the K⁺ cations in $K_3BiAs_6Se_{12}$.

and bridging Se atoms. Every As atom is bonded to an additional terminal Se atom, which lie in equatorial position to the ring. The anion shows C_3 symmetry and is located on a 3-fold axis. Within $[As_3Se_6]^{3-}$ unit, the As–Se bonds are classified into two types. The intra-ring As–Se bond lengths of 2.4317(10) and 2.4437(10) Å are significantly longer than the other As–Se bonds where Se is bound to the Bi^{3+} cation (2.3436(9) Å). The Se–As–Se angles lie between 97.12(3) and 102.48(4)°. The intra-ring As-Se bond lengths and bond angles are comparable with those reported for $[Sr(en)_4]_2(As_3Se_6)Cl$ (en = $C_2N_2H_8$) [34] and $[Mn(dien)_2]_3[As_3Se_6]_2$ (dien = $C_4N_3H_{13}$) [35]. The terminal As–Se bonds are shorter in the latter two compounds compared to that in the title compounds. There are no short Se···Se/As···Se or As···As contacts between the $[As_3Se_6]^{3-}$ anion. The Bi^{3+} cation is in an almost perfect octahedral geometry coordinated by six Se of six different $[As_3Se_6]^{3-}$ units. The lone pair of Bi^{3+} is stereochemically inactive and apparently is delocalized around the Bi nucleus. This is common for Bi^{3+} in an octahedral environment and has been observed in other Bi-Se compounds such as $ABiSe_2$ (A = Na, K) [36,37] and $K_2Bi_8Se_{13}$ [38,39]. Each $[As_3Se_6]^{3-}$ unit serves to bridge three Bi^{3+} ions in the layer using one Se atom per Bi atom. The other three Se atoms remain uncoordinated. The overall arrangement of the Bi^{3+} ions and the $[As_3Se_6]^{3-}$ units resembles the CdI_2 structure type with the cations located on the Cd^{2+} and the anions on the I^- positions, respectively. The Bi–Se bond lengths are almost identical (2.9599(7) to 2.9600(7) Å) and are in the normal range [29]. The Se–Bi–Se angles (see Table 3) clearly demonstrate a very small distortion of the $[BiSe_6]$ octahedron.

The K^+ cations are located between the $^2{}_\infty[Bi(As_3Se_6)_2]^{3-}$ layers. The K(1) ion is coordinated to nine Se atoms in an irregular geometry, whereas K(2) is surrounded by six terminal Se atoms from six $[As_3Se_6]^{3-}$ anions, three above and three below, in a trigonal antiprismatic fashion (Fig. 3). The K–Se distances range from 3.49538(12) to 3.7034(7) Å for K(1)–Se and are 3.2348(8) Å for K(2)–Se. The average K(1)–Se distance is 3.59 Å, corresponding well with the sum of ionic radii (K^+: 1.55 Å (CN = 9); Se^{2-}: 1.98 Å), while the value for K(2)–Se is about 4% shorter than the sum of ionic radii (K^+: 1.38 Å (CN = 6)) [40]. The shortest inter-layer Se–Se distance of 3.755(1) Å is slightly shorter than the sum of the van der Waals radii (3.8 Å).

There are very few known compounds which have a similar structure as the title compound. In $(Me_4N)_2Rb[BiAs_6S_{12}]$ [18], an octahedral Bi^{3+} ion is coordinated by six $[As_3S_6]^{3-}$ groups to form the anionic layers $[Bi(As_3S_6)_2]^{3-}$. Compared to the title compound, the overall arrangement of the Bi^{3+} cations and the $[As_3S_6]^{3-}$ anions in $(Me_4N)_2Rb[BiAs_6S_{12}]$ resembled the $CdCl_2$ structure type, whereas that in the title compound is related to the CdI_2 type. In $Cs_4[Bi(As_2Se_4)(AsSe_3)]$ [29], a distorted octahedral Bi^{3+} cation is coordinated by two *trans*-$[As_2Se_4]^{4-}$ anions and one $[AsSe_3]^{3-}$ moiety. The *trans*-$[As_2Se_4]^{4-}$ anion consists of a cental "$As_2{}^{4+}$" dumbbell where two Se atoms are bonded to each of the As atoms and bridges two Bi^{3+} ions to form a one-dimensional chain $^1{}_\infty[Bi(As_2Se_4)(AsSe_3)]^{4-}$.

3.2. Optical properties

The solid state diffuse reflectance UV/vis spectrum shows a very steep and strong absorption edge at 1.65 eV (Fig. 4) consistent with the black color. The absorption edge is caused by a transition from the top of the valence band (VB) to the bottom of the conduction band (CB), where the upmost part of the valence band can be presumably attributed to Se (3p) states and the bottom of the conduction band results most likely from empty Bi based orbitals. Compared to the band-gap of $RbAg_2As_3Se_6$ which contains also a six-membered $[As_3Se_6]^{3-}$ ring in chair conformation, this data is decreased by ~0.2 eV in title compound.

The far-IR and Raman spectra for $K_3BiAs_6Se_{12}$ in the range from 80 to 550 cm^{-1} are shown in Figs. 5 and 6. The strongest peak in the Raman spectrum at 236 cm^{-1} and the other three weaker resonances at 255, 272, 281 cm^{-1} are comparable to those of $RbAsSe_2$ (240, 263, and 291 cm^{-1}) [12]. The slight shift to lower energy as well as the variation of the intensities is probably related to the covalent interactions between the $[As_3Se_6]^{3-}$ anion and Bi^{3+} cation,

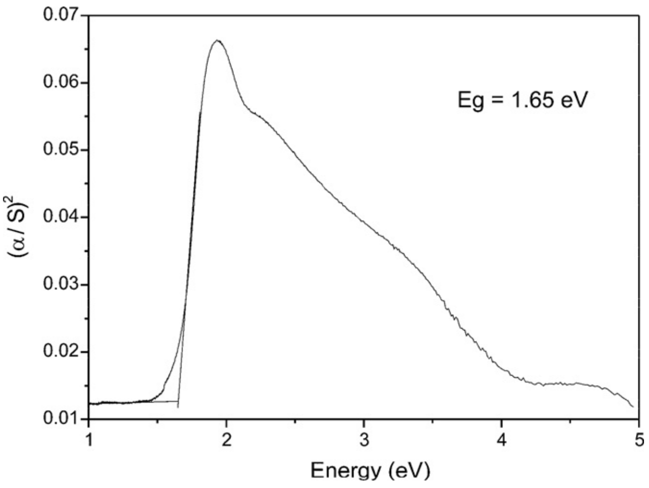

Fig. 4. Transformed reflectance spectrum of $K_3BiAs_6Se_{12}$.

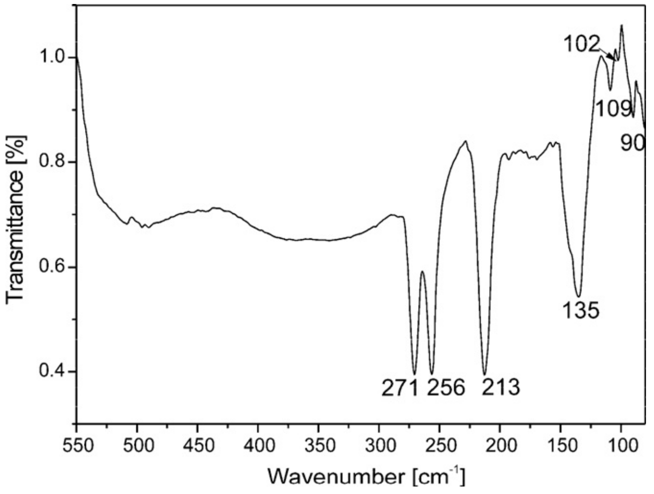

Fig. 5. far-IR spectrum of $K_3BiAs_6Se_{12}$.

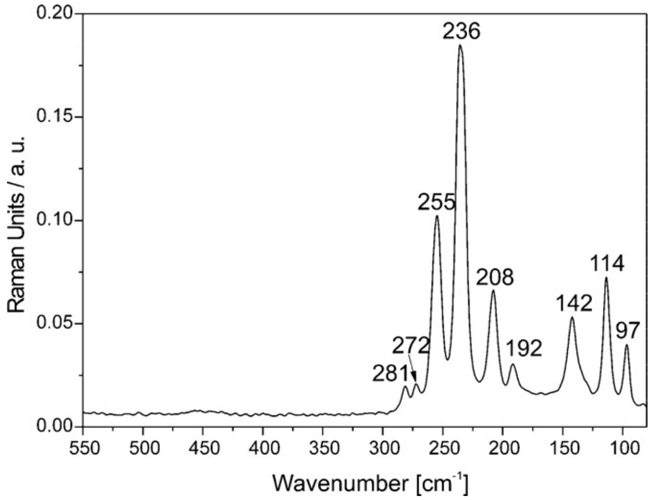

Fig. 6. FT-Raman spectrum of $K_3BiAs_6Se_{12}$.

while there exist $^1{}_\infty[AsSe_2]^-$ chains in $RbAsSe_2$ [41]. This peak and/or the resonance at 281 cm^{-1} are absent in the far-IR spectrum. The two absorptions at 256 and 272 cm^{-1} may be assigned as the antisymmetric ν_{as}(As–Se) stretching vibrations of the $[As_3Se_6]^{3-}$ anion, whereas the peaks at 236 and 281 cm^{-1} are symmetric ν_s(As–Se) vibrations. The resonances at 208 and 192 cm^{-1} in the Raman spectrum and the intense absorption at 213 cm^{-1} in the far-IR spectrum are tentatively assigned as the symmetric ν_s(Bi–Se) and anti-symmetric ν_{as}(Bi–Se) stretching modes, respectively. Compared to the spectra of $K_2AgAs_3Se_6$ [12] these two peaks in the Raman spectrum are shifted to much lower energy. The absorptions between 150 and 80 cm^{-1} in both Raman and IR spectrum may be due to Se–Bi–Se bending vibrations or result from collective lattice modes.

4. Conclusions

The new selenoarsenate $K_3BiAs_6Se_{12}$ was obtained in a reactive flux using As_2Se_3 as the selenoarsenate source. The layered anion $^2{}_\infty[Bi(As_3Se_6)_2]^{3-}$ contains octahedrally coordinated Bi^{3+} cations and the crown-like anion $[As_3Se_6]^{3-}$. The compound $K_3BiAs_6Se_{12}$ was synthesized in a selenium-rich potassium polyarsenate flux with relative low Lewis basicity. These conditions seem to be essential for the stabilization of the compound because increasing the flux basicity results in the breakdown of the structure and formation of simpler compounds. Although the synthesis of compounds containing specific ligands $[As_xSe_y]^{n-}$ would be hard to control interesting compounds can be expected applying fluxes with different compositions and properties.

Acknowledgement

Financial support by the DFG (Deutsche Forschungsgemeinschaft) is gratefully acknowledged.

Appendix A. Supplementary data

Supplementary data associated with this article can be found, in the online version, at doi:10.1016/j.jallcom.2011.01.108.

References

[1] W.S. Sheldrick, M. Wachhold, Coord. Chem. Rev. 176 (1998) p211.
[2] V. Vater, W.S. Sheldrick, Z. Naturforsch. B 53 (1998) p1259.
[3] M. Wachhold, W.S. Sheldrick, Z. Naturforsch. B 52 (1997) p169.
[4] M. Wachhold, W.S. Sheldrick, Z. Naturforsch. B 51 (1996) p32.
[5] G. Cordier, C. Schwidetzky, H. Schafer, Z. Naturforsch. B 40 (1985) p1.
[6] T.K. Bera, J.I. Jang, J.B. Ketterson, M.G. Kanatzidis, J. Am. Chem. Soc. 131 (2009) p75.
[7] T.K. Bera, M.G. Kanatzidis, Inorg. Chem. 47 (2008) p7068.
[8] T.K. Bera, R.G. Iyer, C.D. Malliakas, M.G. Kanatzidis, Inorg. Chem. 46 (2007) p8466.
[9] R.G. Iyer, J. Do, M.G. Kanatzidis, Inorg. Chem. 42 (2003) p1475.
[10] M. Wachhold, M.G. Kanatzidis, Inorg. Chem. 39 (2000) p2337.
[11] M. Wachhold, M.G. Kanatzidis, Inorg. Chem. 38 (1999) p4178.
[12] M. Wachhold, M.G. Kanatzidis, Inorg. Chem. 38 (1999) p3863.
[13] J.A. Hanko, J.H. Chou, M.G. Kanatzidis, Inorg. Chem. 37 (1998) p1670.
[14] J.H. Chou, J.A. Hanko, M.G. Kanatzidis, Inorg. Chem. 36 (1997) p4.
[15] M.G. Kanatzidis, J.H. Chou, J. Solid State Chem. 127 (1996) p186.
[16] J.H. Chou, M.G. Kanatzidis, J. Solid State Chem. 123 (1996) p115.
[17] J.H. Chou, M.G. Kanatzidis, Inorg. Chem. 33 (1994) p5372.
[18] J.H. Chou, M.G. Kanatzidis, Inorg. Chem. 33 (1994) p1001.
[19] G.L. Schimek, J.W. Kolis, Acta Cryst. C 53 (1997) p991.
[20] J.E. Jerome, P.T. Wood, W.T. Pennington, J.W. Kolis, Inorg. Chem. 33 (1994) p1733.
[21] S.C. Oneal, W.T. Pennington, J.W. Kolis, Inorg. Chem. 31 (1992) p888.
[22] S.C. Oneal, W.T. Pennington, J.W. Kolis, J. Am. Chem. Soc. 113 (1991) p710.
[23] F. Pertlik, Monatsh. Chem. 125 (1994) p1311.
[24] F. Pertlik, J. Solid State Chem. 112 (1994) p170.
[25] R.G. Iyer, M.G. Kanatzidis, Inorg. Chem. 41 (2002) p3605.
[26] Y.D. Wu, C. Näther, W. Bensch, Inorg. Chem. 45 (2006) p8835.
[27] Y.D. Wu, W. Bensch, Solid State Sci. 11 (2009) p1542.
[28] Y.D. Wu, W. Bensch, Inorg. Chem. 48 (2009) p2729.
[29] M. Wachhold, M.G. Kanatzidis, Z. Anorg, Allg. Chem. 626 (2000) p1901.
[30] L. Iordanidis, M.G. Kanatzidis, J. Am. Chem. Soc. 122 (2000) p8319.
[31] G.M. Sheldrick, Acta Cryst. A 64 (2008) p112.
[32] A.L. Spek, J. Appl. Crystallogr. 36 (2003) p7.
[33] P. Kubelka, F. Munk, Z. Tech. Phys. 12 (1931) p593.
[34] W.S. Sheldrick, J. Kaub, Z. Naturforsch. B 40 (1985) p1020.
[35] M.L. Fu, G.C. Guo, X. Liu, B. Liu, L.Z. Cai, J.S. Huang, Inorg. Chem. Commun. 8 (2005) p18.
[36] G. Gattow, J. Zemann, Z. Anorg, Allg. Chem. 279 (1955) p324.
[37] B. Eisenmann, H. Schafer, Z. Anorg, Allg. Chem. 456 (1979) p87.
[38] T.J. McCarthy, S.P. Ngeyi, J.H. Liao, D.C. Degroot, T. Hogan, C.R. Kannewurf, M.G. Kanatzidis, Chem. Mater. 5 (1993) p331.
[39] D.Y. Chung, K.S. Choi, L. Iordanidis, J.L. Schindler, P.W. Brazis, C.R. Kannewurf, B.X. Chen, S.Q. Hu, C. Uher, M.G. Kanatzidis, Chem. Mater. 9 (1997) p3060.
[40] R.D. Shannon, Acta Cryst. A 32 (1976) p751.
[41] W.S. Sheldrick, H.J. Häusler, Z. Anorg, Allg. Chem. 561 (1988) p139.